

N 9 1 - 1 7 7 2 4 1

# Current Collection by High Voltage Anodes in near Ionospheric Conditions

J. A. Antoniadis, R. G. Greaves, D. A. Boyd and R. Ellis  
University of Maryland  
College Park, MD.

## Introduction

In the absence of neutral gas breakdown in the vicinity of an orbital or suborbital vehicle the spacecraft charging potential of the vehicle is primarily determined by the current collection from the ambient plasma as well as the energetic particle flux incident on it. In the presence of a low pressure neutral background and a weak magnetic field the current collection behavior can be strongly modified due to electrical discharges in the vicinity of a high voltage electrode. These discharges usually produce large amounts of plasma in the surrounding region of the electrode, which overwhelms the ambient plasma environment resulting in highly modified current collection and large scale high current glow discharges. In situations where the system size is larger than the local Parker-Murphy radius, [1] the neutral pressure required for the breakdown is usually far below the pressure at the Paschen minimum.

For positively charged conductors the main cause for the discharges is electron trapping in magnetic bottles formed in the vicinity of the anode by the combination of the anode's electric field and the ambient axial magnetic field. The magnetic bottle boundaries have been discussed in the work of Rubinstein and Laframboise. [2] The existence of these bottles has been verified experimentally by Greaves et al. [3] Trapping of electrons can lead to the initiation of ionization cascades resulting in breakdown. The breakdown criteria for this type of discharge have been treated analytically in a theory by Kunhardt et al. [4]

We have experimentally identified three distinct regimes with large differences in current collection in the presence of neutrals and weak magnetic fields. In magnetic field/anode voltage space the three regions are separated by very sharp transition boundaries. We performed a series of laboratory experiments to study the dependence of the region boundaries on several parameters, such as the ambient neutral density, plasma density, magnetic field strength, applied anode voltage, voltage pulsewidth, chamber material, chamber size and anode radius.

The three observed regimes are:

- Classical magnetic field limited collection
- Stable medium current toroidal discharge
- Large scale, high current space glow discharge

There is as much as several orders of magnitude of difference in the amount of collected current upon any boundary crossing, particularly if one enters the space glow regime. We measured some of the properties of the plasma generated by the breakdown that is present in regimes II and III in the

vicinity of the anode including the sheath modified electrostatic potential, I-V characteristics at high voltage as well as the local plasma density.

## Experiments and Diagnostics

The low neutral pressure discharges were initially observed during the **Space Power Experiments Aboard Rockets (SPEAR I)** vacuum chamber tests at the University of Maryland and NASA Plum Brook station by Antoniadis et al. [5, 7, 9] They were then reproduced and studied in more detail at the University of Maryland SPIE chamber by Alport et al. [6]

Figure 1 shows a schematic diagram of the Maryland SPIE chamber where the majority of the experiments were conducted. SPIE is a cylindrical vacuum chamber 1.8 m diameter, 5 m long constructed entirely of non-magnetic stainless steel. The chamber can be evacuated to  $5 \times 10^{-7}$  Torr with a combination of a turbomolecular and a cryogenic pump. A multi-dipole plasma source is capable of filling the chamber with cold plasmas of varying ion species, but mainly with argon and nitrogen. The plasma density in the main chamber can be varied between  $10^8 - 10^{13} \text{ m}^{-3}$ . Typical plasma electron temperatures are in the range of 1 - 3 eV.

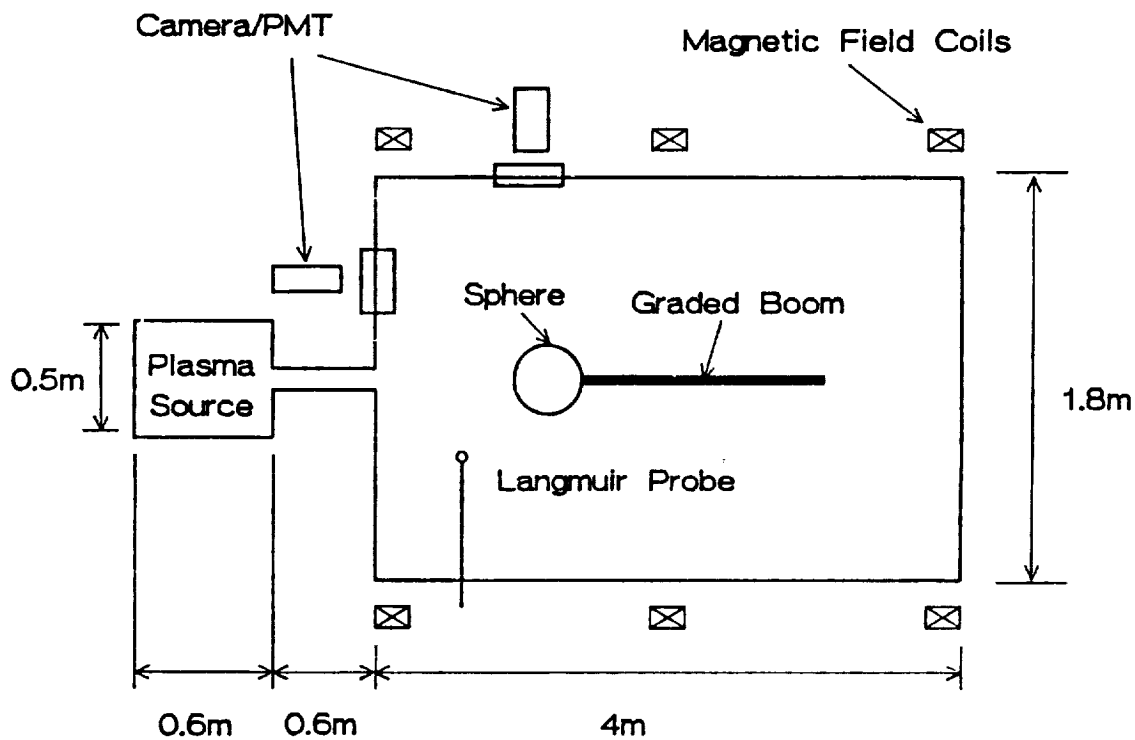


*Figure 1 : Schematic diagram of the SPIE chamber (Only the axial magnetic field coils are shown).*

Two sets of magnetic field coils surround the chamber. One set can apply transverse magnetic fields but is primarily used to cancel the earth's

magnetic field inside the chamber while the other allows the application of an axial magnetic field in the range of .1-36 Gauss. The anodes consisted of several high voltage spheres ranging in radius from 1 - 10 cm.

The NASA Plum Brook B-2 chamber is a 13 m diameter 20 m long cylindrical vacuum chamber. The chamber can be pumped to  $1 \times 10^{-6}$  Torr with 12, 36" diffusion pumps. It was also filled with plasma to densities comparable to the peak plasma density in the LEO environment (up to  $5 \times 10^6 \text{ cm}^{-3}$ ). Only one sphere was present for the mockup tests instead of the two spheres that were actually flown in the SPEAR I Mission.[7] A capacitive discharge system was used to apply the high voltage pulses to the sphere. When a low impedance glow discharge was initiated the pulse RC decay time was 4 msec with a maximum output current  $\approx 11$  Amps. When no discharge was present the pulse decay time was 1 sec. Figure 2 shows a schematic diagram of the capacitive discharge pulse circuit.

Several diagnostics were utilized during the experiments. Single electric probes with an assortment of tips were used to measure the electron density and temperature. Hot filament emissive probes were used to

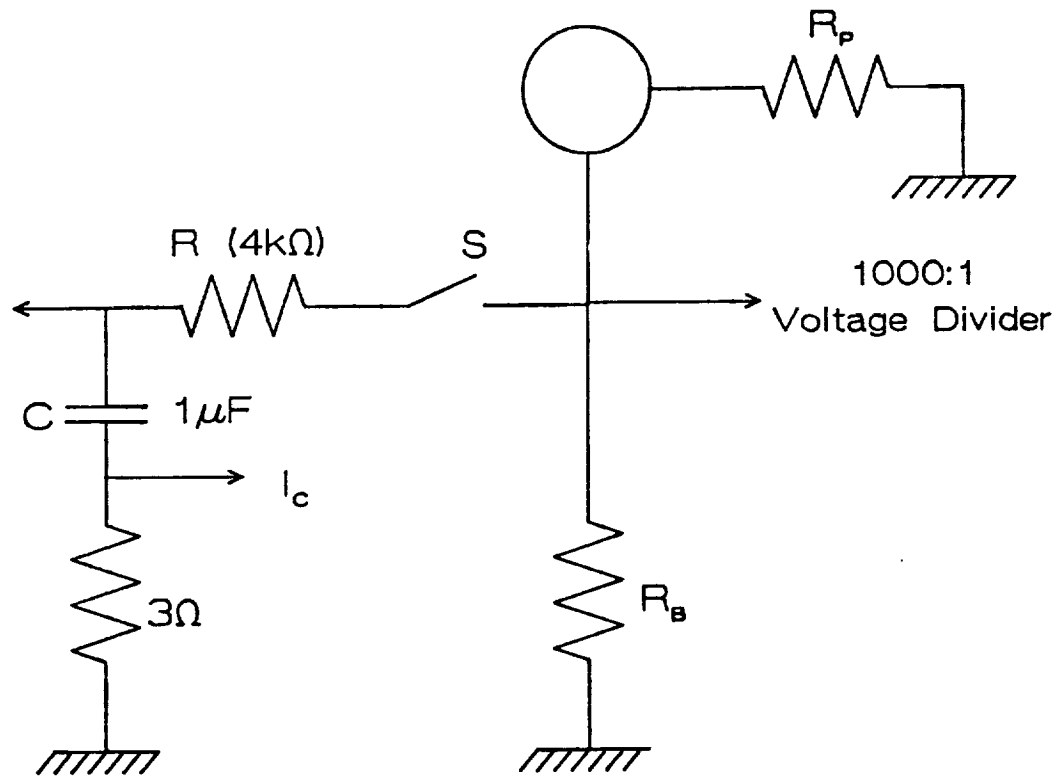


*Figure 2. Schematic diagram of the capacitive discharge circuit for the current collection experiments. When the plasma impedance  $R_p$  is large (no breakdown) the RC decay time constant is 1 sec, but when breakdown occurs the RC time drops to 4 msec.*

measure the plasma potential inside the discharge itself. The time-dependent evolution of the wavelength-integrated visible light emission from the discharge was measured with cooled photomultiplier tubes. An ion energy analyzer measured the ion spectra for the ballistic ions ejected from the discharge. A set of isolated metallic plates near the outside wall was used to measure the time-resolved wall current distribution during all phases of the discharge. Video and photographic equipment, 35 mm and a video cameras were used to photograph the discharges. The main power system was monitored by a resistive voltage divider measuring the applied voltage and a two current shunts to measure the current collected by the sphere and the specially shielded graded support boom.

## Results

Figure 3 shows a typical breakdown region diagram in Anode Voltage/Magnetic field space. Region I differs from the other two in that there is no self-sustaining discharge in the anode vicinity. Regions II and III are distinctly different because the system collection characteristics are dominated by the plasma resulting from breakdown of the ambient neutral gas. Region II is the "Space Glow" regime where very large currents were drawn by the anode limited seemingly by the current capability of our pulse discharge system. Region III is the "Torus" regime where the anode is surrounded by a steady state toroidal discharge as shown in figure 4. The current drawn by the anode in region III lies between the currents in regions I and II. The location of the boundaries separating the discharge regions is a function of the ambient neutral pressure, electron trapping efficiency, anode size and ambient plasma density. The region boundaries represent very sharp transitions in collected current and optical emission in the vicinity of the anode. They are also very sharply dependent on magnetic field, so that B field changes of  $< 0.1$  Gauss can result in a boundary crossing.

Figure 5 shows a typical set of time resolved diagnostic traces for a space glow formation. The top trace shows the visible light intensity, the center trace shows the current collected by the anode and the bottom trace shows the anode voltage. The light emission from the cascade initiation in the vicinity of the anode starts several hundred microseconds before any noticeable effects are observed in the anode current or voltage. The light intensity initially rises exponentially but when the cascades develop further it rises faster than a simple exponential. The drop in the anode voltage and the apparent current saturation in this figure are due to a current limiting series resistor in the driving circuit to prevent catastrophic arcs from occurring.

Figure 6 shows the dependence of the discharge formation time when the axial magnetic field is varied. The background neutral pressure is  $2 \times 10^{-5}$  Torr. This figure demonstrates the sharpness of the dependence of the breakdown threshold on magnetic field since it shows that a field change of 0.05 Gauss can reduce the time for discharge initiation from practically infinity to less than 1 msec.

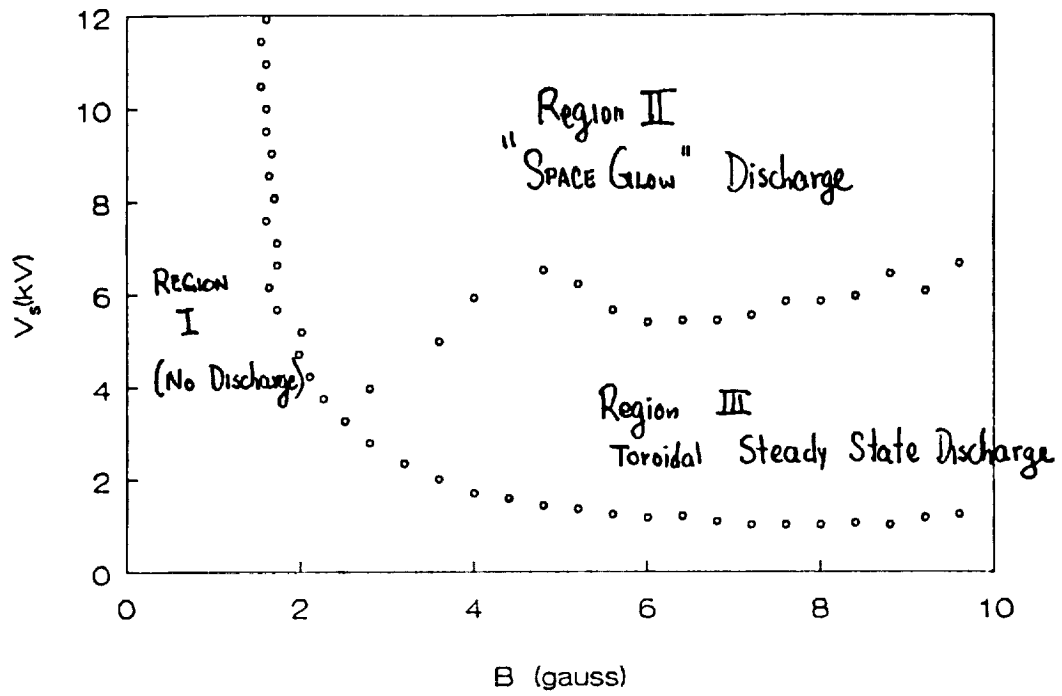


Figure 3. Discharge region diagram in Magnetic field vs Anode voltage space for neutral pressure is  $2 \times 10^{-5}$  Torr and no ambient plasma injection.

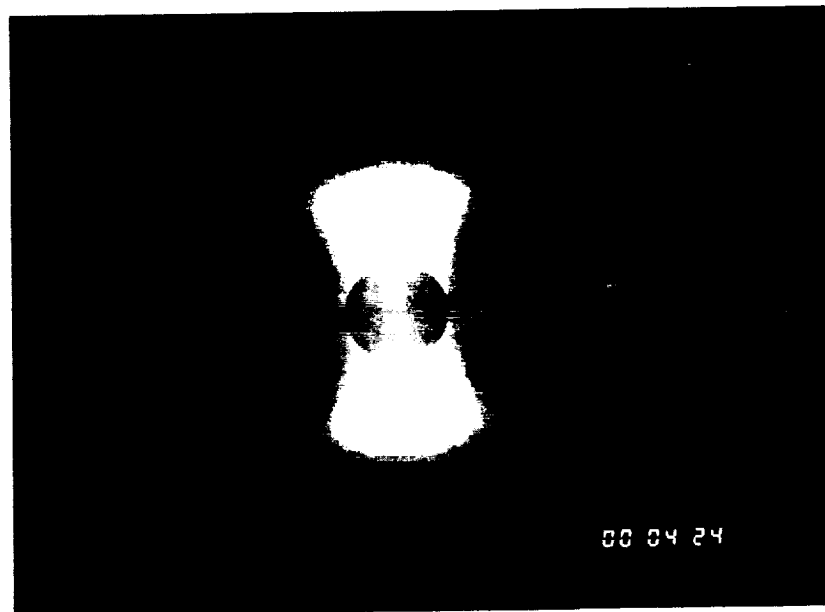


Figure 4. Photograph of the plasma filled torus that is generated by the trapped electrons.

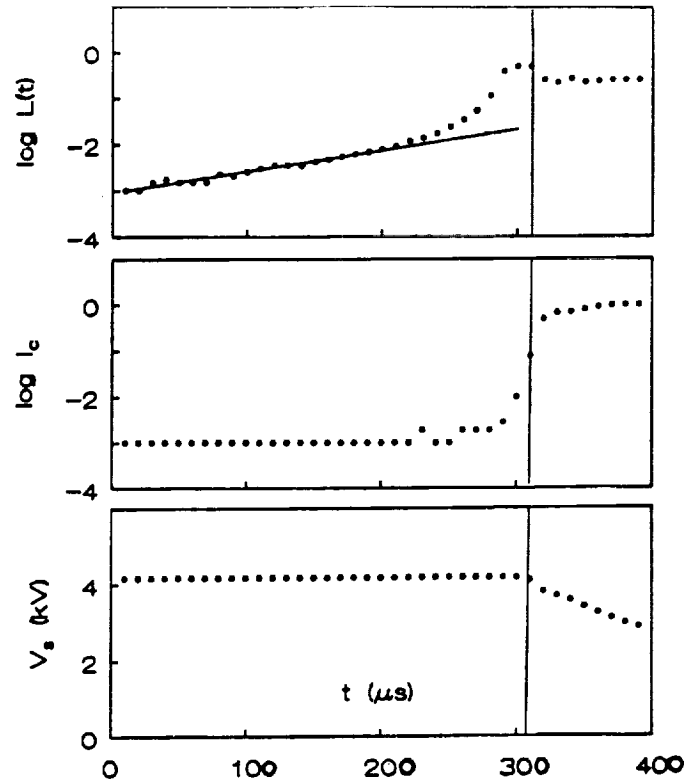


Figure 5. Waveforms for the wavelength-integrated optical light emission, anode current and anode voltage. The low level light emission starts well before any detectable effects are observed in the other diagnostics.

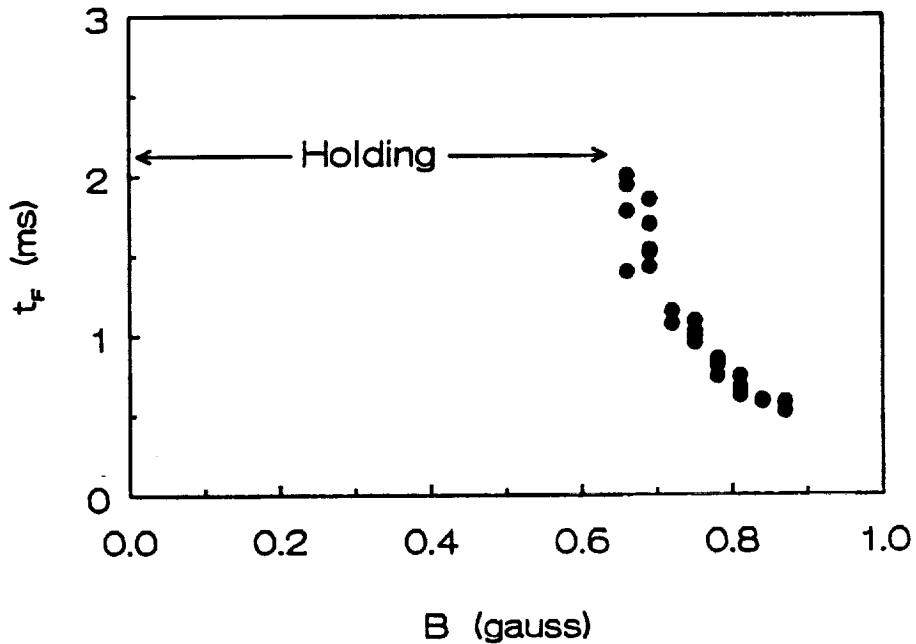


Figure 6. Discharge formation time vs axial magnetic field. For magnetic fields below the critical value no self-sustaining discharge is formed even when a DC high voltage is applied to the anode.

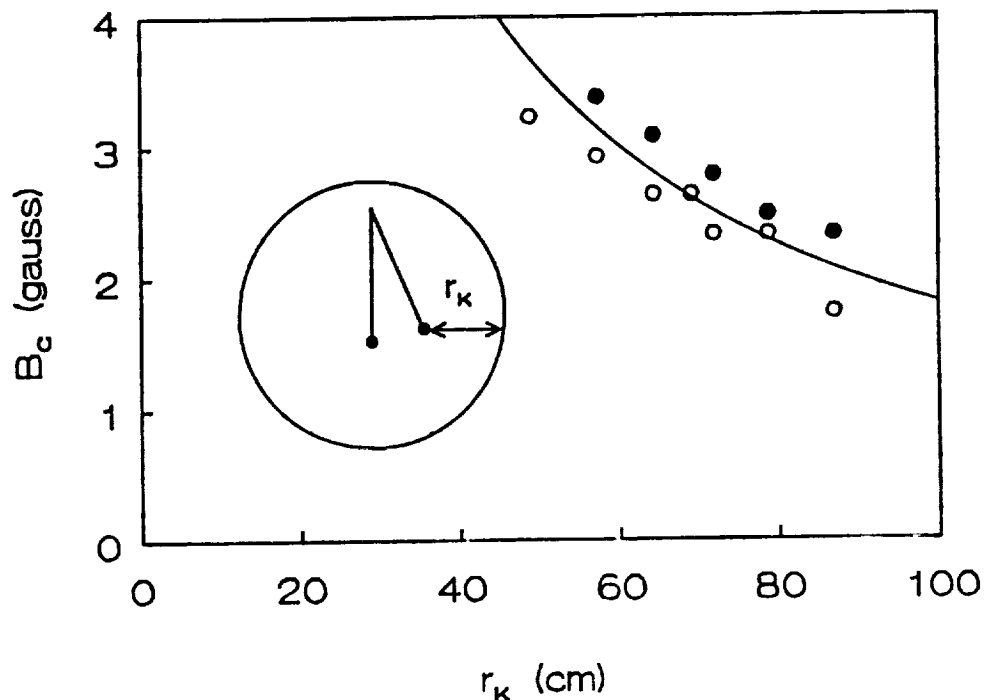


Figure 7. The critical magnetic field for discharge initiation is shown as a function of the chamber size. The neutral pressure is  $2 \times 10^{-5}$  Torr.

When an ambient plasma is introduced into the chamber the discharge formation time decreases sharply with increasing plasma density. In addition the magnetic field threshold for a discharge to occur is also reduced compared to the case without an ambient plasma.

The proximity of the walls plays a major role in the breakdown initiation and discharge gain. Figure 7 shows the critical magnetic field, that is the value of magnetic field below which no breakdown is observed, as a function of the anode to cathode radius. In these experiments this is accomplished by swinging the anode closer to the chamber wall. The critical field increases with decreasing radius, which is consistent with the trapping picture since higher magnetic fields are required to reduce the size of the magnetic bottles to fit into the smaller chamber.

Figure 8 shows the axial dependence of the currents perpendicular to the magnetic field in a region III discharge. The vertical axis represents the ratio of the current at an some axial position divided by the current at  $z=0$ , which is in the midplane of the anode and perpendicular to the magnetic field. The two curves in the figure correspond to magnetic field values of 5 Gauss and 15 Gauss. As the magnetic field increases the wall current distribution becomes more strongly peaked at the midplane. The optical and probe measurements indicate that the torus plasma density is peaked at the midplane and since the ions are unmagnetized, they are ejected radially

outwards resulting at a higher ion flux and secondary electron flux at the wall at the midplane and thus a peaked wall current profile.

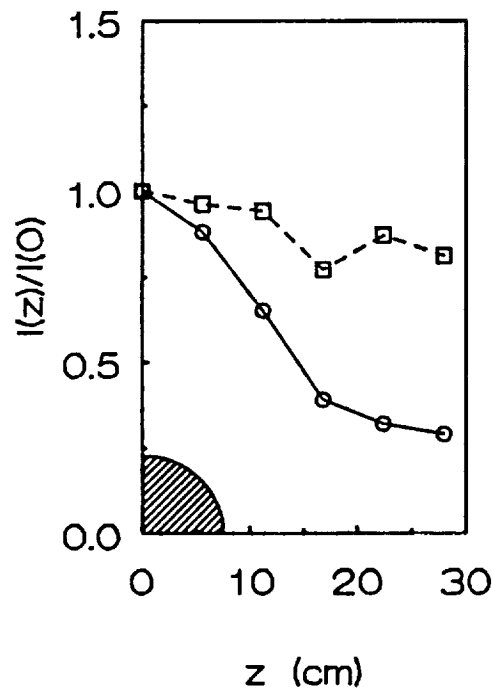


*Figure 8. Wall current distribution for 5 and 15 Gauss applied axial magnetic field. The wall current is the sum of the incident ion current and the secondary electron current.*

The shape of the potential sheath around the anode during a steady state torus regime discharge was measured using an emissive electric probe. The potential vs radius for 5 and 15 Gauss axial field shown in figure 9. It is important to notice that the sheath radius decreases with increasing magnetic field and a large flat potential region separates the sheath from the chamber wall. It is also apparent that there are small local potential wells near the edges of the sheath signaling the possible existence of thin double layers.

Figures 10 and 11 show the collected current dependence on pressure and anode voltage for discharges in the torus regime. For pressures below  $1 \times 10^{-5}$  Torr the collected current is directly proportional to the ambient neutral pressure, but as the pressure increases the dependence becomes exponential and eventually the current increases dramatically when the pressure increases to initiate a space glow discharge. The current-voltage characteristics are much more complicated with the slope of the I-V curve



changing significantly as a function of voltage even exhibiting hysteresis and negative resistance regions especially when a background plasma is present.[8]

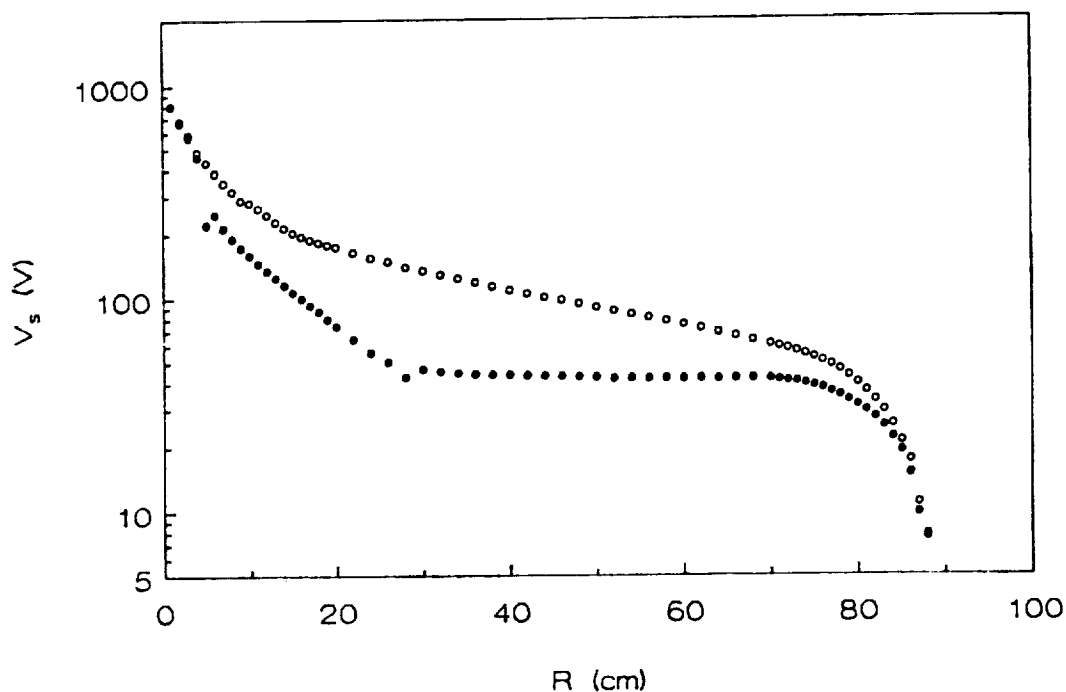


*Figure 9. The radial potential distribution for a 7.5 cm diameter anode in the presence of the region III torus measured with an emissive electric probe. The curves correspond to magnetic fields of 5 and 15 Gauss.*

## Discussion

The increase in current collection in the presence of a neutral background is due to electron trapping in the region surrounding the anode in the presence of a magnetic field. Electrons are trapped by a combination of  $E \times B$  trapping and electrostatic trapping. The  $E \times B$  trapping is due to the electric field of the anode crossed with the ambient magnetic field. The electrostatic trapping is due to the axial variation of the electrostatic potential of the charged anode. As the calculations of Rubinstein and Laframboise [2] show, the electrons are trapped in magnetic bottles and they can only be collected only when they are scattered into a bottle that comes in contact with the anode surface. Electron scattering can result from collisions with the background neutrals or sheath turbulence [9]. The magnetic bottles have scale lengths of the order of the Parker-Murphy radius so in order for breakdown to

occur the chamber radius must be larger than the P-M radius since trapping is destroyed if a magnetic bottle comes in contact with the chamber wall. This is the reason for the increase in critical magnetic field for a decrease in chamber radius. Thus even though the mean free path for electron-neutral collisions in this regime is very much longer than the anode-cathode distance, the effective path length of a collected electron can exceed the mean free path for collisions. Long path trajectories give rise to very high gain ionization cascades, thus driving the system to a glow discharge mode even at the extremely low neutral pressures far below the Paschen breakdown curve. The ions generated by ionization cascades are unmagnetized in low values of magnetic field and are accelerated by the anode potential hill and ballistically ejected in the radial direction. When these ions impact the chamber wall they release secondary electrons that enter the discharge and produce more ionization cascades leading to high current breakdown when the ionization rate exceeds the electron detrapping rate. It is also theoretically shown by Kunhardt [4] that this type of breakdown is also possible if the secondary emission from a wall is replaced by the thermal electron current collected through a sheath when the entire system is surrounded by a large plasma as is the case in the ionosphere.

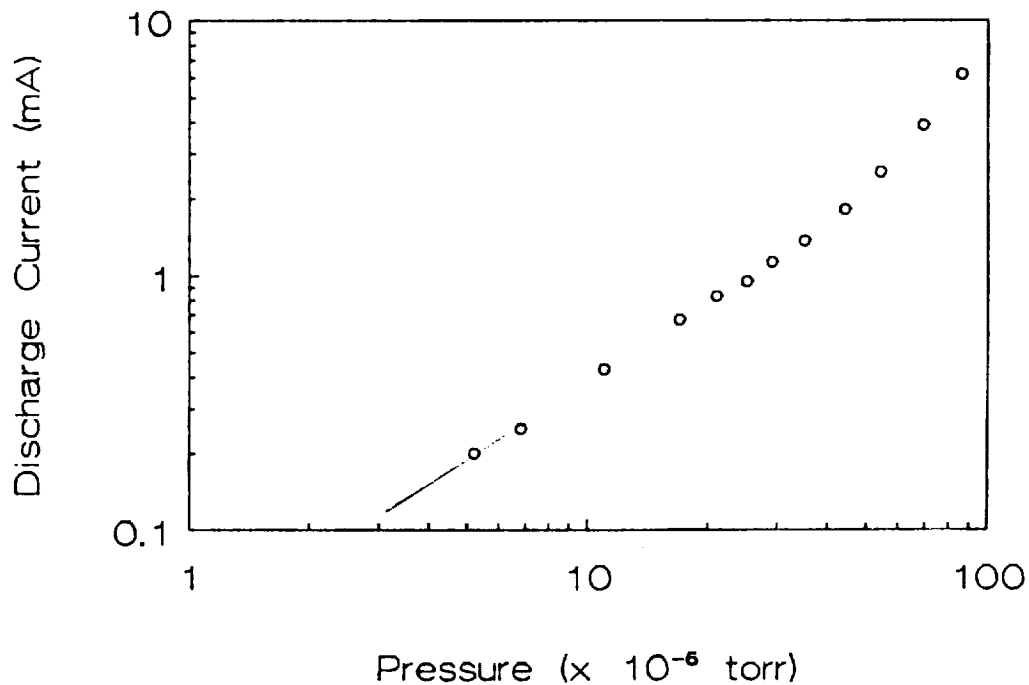


*Figure 10. Anode current collection for a constant magnetic field as a function of the ambient neutral pressure. Further pressure increase above  $1 \times 10^{-4}$  Torr results in a high current glow discharge.*

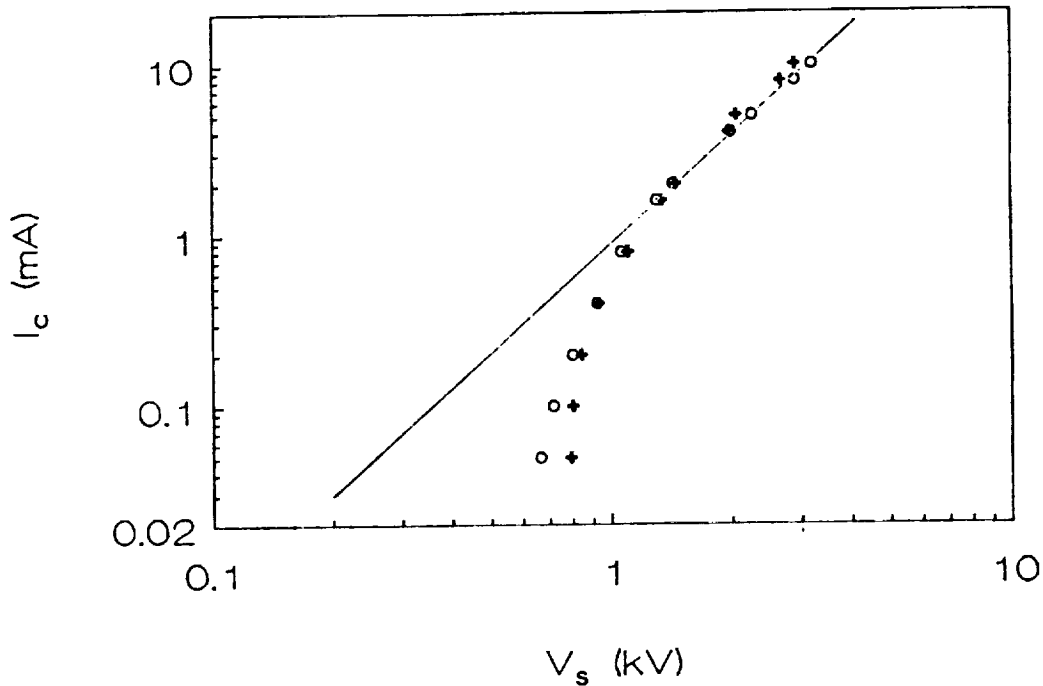


*Figure 11. Anode current vs applied voltage for fixed magnetic field and ambient neutral pressure.*

## Conclusions

In the presence of a low pressure neutral background in the vicinity of an anode charged to voltages as low as several hundred volts highly enhanced current collection due to large scale diffuse breakdown is possible in a weakly magnetized system. The neutral gas pressure required for breakdown initiation is usually far below the value of the Paschen curve and corresponds to pressures identified as "high vacuum". Even though for many space applications discharges are undesirable, there are situations such as spacecraft "grounding" or electromagnetic tethers where high collection currents are necessary. These discharges which are diffuse in nature offer possible alternatives to hollow cathodes, hot filaments or charged particle guns for those types of applications that require sustained high current collection.

This Research was supported by the Strategic Defense Initiative Office of Innovative Science and Technology through the Office of Naval Research.

## References

- [1] L. W. Parker and B. L. Murphy, "Potential Buildup on an electron-emitting satellite", *Journal of Geophysical Research*, Vol. 72, 1967, pp. 1631-1636.
- [2] J. Rubinstein and J. G. Laframboise, *Phys. Fluids* 25, 1982, pp. 1174-1182.
- [3] R. G. Greaves, D. A. Boyd, J. A. Antoniadis and R. F. Ellis, "Steady-State Toroidal Plasma around a Spherical Anode in a Magnetic Field", *Phys. Rev. Lett* 64, #8, 1990, pp. 886-889
- [4] E. E. Kunhardt, S. Lederman, E. Levi, G. Schaefer, W. C. Nunnally, W. E. Dillon and C. V. Smith, "Electrical Breakdown of the Insulation Properties of the Space Environment", *Proceedings of the XIII International Symposium on Discharges and Electrical Insulation in Vacuum*, Paris, 1988, pp. 247-249
- [5] J. A. Antoniadis, M. J. Alport, D. A. Boyd and R. F. Ellis, "Vacuum Chamber Ground Testing of the SPEAR I Exposed High Voltage Components", *IEEE Transactions on Electrical Insulation*, to be published, June 1990
- [6] M. J. Alport, J. A. Antoniadis, D. A. Boyd, R. G. Greaves and R. F. Ellis, "Electrical Breakdown at Low Pressure in a Weak Magnetic Field", *Journal of Geophysical Research*, to be published, Spring 1990
- [7] D. B. Allred et al., "The SPEAR I Experiment, High Voltage Effects on Space Charging in the Ionosphere", *IEEE Transactions on Nuclear Science*, Vol. 35, 1988, pp. 1386-1393
- [8] J. A. Antoniadis, R. G. Greaves, D. A. Boyd and R. F. Ellis, "Current Collection in Near Ionospheric Conditions in the Presence of Neutrals", *Reprint from the 28th Aerospace Sciences AIAA Meeting*, Reno, 1990, #90-0632
- [9] P. Palmadesso, *Private Communication*.